APPLIED PHYSICS LETTERS **89**, 131913 (2006)

Concentration dependence of carrier localization in InN epilayers

G. W. Shu, P. F. Wu, M. H. Lo, and J. L. Shen[a)]
Physics Department, Chung Yuan Christian University, Chung-Li, Taiwan 32023, Republic of China

T. Y. Lin
Institute of Optoelectronic Sciences, National Taiwan Ocean University, Keelung, Taiwan 20224, Republic of China

H. J. Chang and Y. F. Chen
Physics Department, National Taiwan University, Taipei, Taiwan 106, Republic of China

C. F. Shih
Electrical Engineering Department, National Cheng Kung University, Tainan, Taiwan 70101, Republic of China

C. A. Chang and N. C. Chen
Optoelectronic Engineering Institute, Chang Gung University, Guei-Shan, Taiwan 33302, Republic of China

(Received 27 April 2006; accepted 8 August 2006; published online 27 September 2006)

The authors studied the concentration dependence of carrier localization in InN epilayers using time-resolved photoluminescence (PL). Based on the emission-energy dependence of the PL decays and the PL quenching in thermalization, the localization energy of carriers in InN is found to increase with carrier concentration. The dependence of carrier concentration on the localization energy of carriers in InN can be explained by a model based on the transition between free electrons in the conduction band and localized holes in the deeper tail states. They suggest that carrier localization originates from the potential fluctuations of randomly located impurities. © *2006 American Institute of Physics*. [DOI: 10.1063/1.2357545]

InN has recently attracted extensive attention due to its potential applications in semiconductor devices such as light-emitting diodes, lasers, and high efficiency solar cells. As of yet, many intrinsic electronic properties of InN, such as the energy band gap, the electron effective mass, and nonparabolicity of the conduction band, have not been fully understood.[1–6] The photoluminescence (PL) of degenerate InN has recently been studied and the PL structures have been analyzed by recombination processes of the free-to-bound, free-to-tail, and band-to-band transitions.[5,6] The PL spectra in InN have been found to exhibit the carrier localization because the energy relaxation time of photoexcited carriers is much shorter than the radiative lifetime.[5] The origin of the localized states has been associated with the spatial fluctuations of random impurity potential[5,6] or metallic indium inclusions.[7] The intrinsic material properties of InN are well known to be very sensitive to the presence of impurities, i.e., carrier concentration. Therefore, it is desirable to investigate the concentration-dependent carrier localization in InN, which will not only improve the understanding of the material properties of InN but also provide information on the design of InN-based devices. In this study, we investigate the concentration dependence of carrier localization in InN. We suggest that carrier localization in InN originates from the potential fluctuations of randomly located ionized impurities.

The samples investigated were grown on sapphire substrates by metal organic vapor phase epitaxy. A low-temperature 20 nm GaN nucleation layer was firstly deposited at 500 °C, followed by a 2 μm GaN layer grown at 1000 °C. The substrate was then cooled to 600 °C to grow the InN. Trimethyl indium (TMI) and NH_3 were used as sources and N_2 was used as the carrier gas at flow rates of 400, 18 000, and 18 000 SCCM (SCCM denotes cubic centimeter per minute at STP) for TMI, NH_3, and N_2, respectively. The pressure during growth was kept constant at 200 mbars. An InN layer with a thickness of 150 nm was grown on the GaN layer. Various electron concentrations were obtained by varying the temperature of rapid thermal annealing (RTA) in an O_2 environment. RTA was performed with an annealing time of 30 s and a ramp rate of 30 °C/s at temperatures of 200, 300, 400, and 500 °C for samples D, C, B, and A, respectively (sample E was untreated). The InN samples A, B, C, D, and E with carrier concentrations of 2.4, 3.3, 9.0×10^{18}, 1.4, and 1.6×10^{19} cm^{-3}, respectively, were obtained from the Hall effect measurements at room temperature. The PL measurements were performed using a pulsed laser operating at a wavelength of 635 nm as the excitation source. The pulsed laser produces light pulses with 50 ps duration and a repetition rate of 1 MHz. The luminescence was detected with an extended InGsAs detector or a high-speed photomultiplier tube. PL decay signals were measured using the technique of time-correlated single-photon counting. The overall temporal response function of the system is 250 ps.

The dashed lines in Fig. 1 display the 10 K PL of five InN samples with different free carrier concentrations. The energy of the PL increases monotonically as the electron concentration increases. The blueshift of the PL peak is caused by the Burstein-Moss effect originating from the shift of the Fermi level above the bottom of the conduction band as the electron concentration increases.[8] Figure 2 displays the PL decay profiles of InN monitored at the peak position with

[a)]Author to whom correspondence should be addressed; electronic mail: jlshen@cycu.edu.tw

 © 2006 American Institute of Physics
Downloaded 19 Oct 2008 to 140.116.208.51. Redistribution subject to AIP license or copyright; see http://apl.aip.org/apl/copyright.jsp

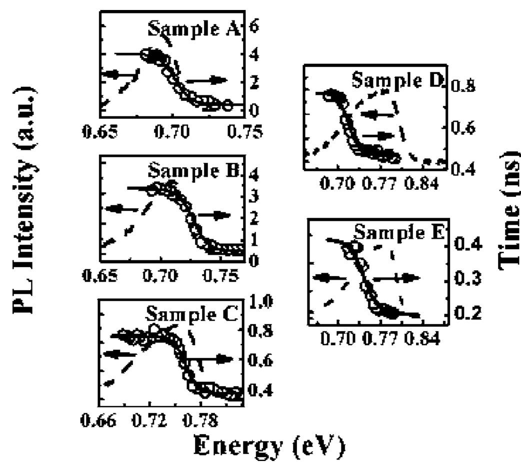

FIG. 1. PL spectra of five InN samples with different free carrier concentrations (dashed lines). The open circles display the emission-energy dependence of lifetime τ. The solid lines display the calculated τ using Eq. (1).

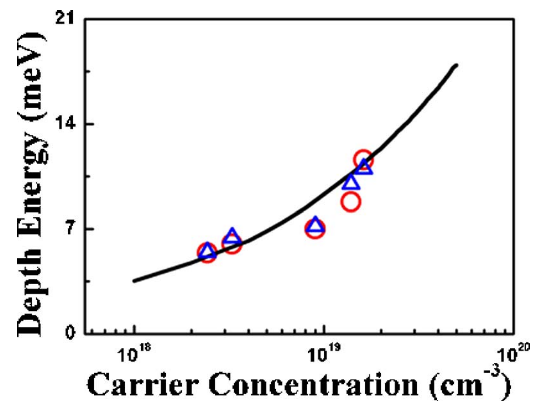

FIG. 3. (Color online) Localization energy E_0 obtained from Eq. (1) (open circles) and the activation energy E_2 obtained from Eq. (2) (open triangles) as functions of carrier concentration. The solid line plots the calculated localization energy according to a model that considers the potential fluctuations of impurities.

different carrier concentrations. Each PL transient profile in Fig. 2 can be fitted by the function $I(t)=I_0\exp(-t/\tau)$, where τ is the decay lifetime. A carrier lifetime as long as 3.7 ns was observed for sample A. This value is the longest lifetime measured to date for InN.[9]

The open circles in Fig. 1 show the emission-energy dependence of lifetime τ with five different carrier concentrations. The decrease of the lifetimes with increasing emission energy is characteristic of a localization effect.[10] Localized carriers can transfer from higher energy sites to lower energy sites through a relaxation. The decay rate of localized carriers is expressed as the radiative recombination rate plus the transfer rate to lower energy sites. Thus, the observed lifetime decreases as the emission energy increases. The combination of recombination and transfer has been modeled by assuming that the density of localized tail states is proportional to $\exp(-E/E_0)$, where E_0 describes the amount of spreading in the density of states.[11,12] The relationship between lifetime τ and PL energy E is described by the function[12]

$$\tau=\frac{\tau_{\mathrm{rad}}}{1+\exp[(E-E_{\mathrm{me}})/E_0]}, \qquad (1)$$

where τ_{rad} is the radiative lifetime, E_{me} is an energy where the decay time equals the transfer time, and E_0 is the localization energy. τ given by Eq. (1) is plotted as the solid lines in Fig. 1. Good fits to experimental data confirm the existence of carrier localization in InN. The open circles in Fig. 3 plot E_0 with five different carrier concentrations. E_0 decreases monotonically with a decrease of carrier concentration; this behavior will be discussed later.

The PL intensity of InN as a function of temperature was measured and the open circles in Fig. 4 show the experimental results for five different carrier concentrations. The PL intensities decrease monotonically with temperature. An attempt to fit the Arrhenius plots of the PL emission using the dependence of $A(T)=A_0/[1+C\exp(-E_A/kT)]$ was unsuccessful (see the dashed lines in Fig. 4). However, the temperature-dependent PL intensities can be well fitted by two nonradiative recombination channels using the function[13]

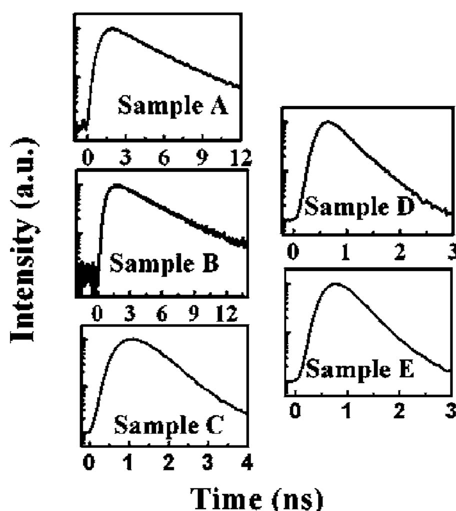

FIG. 2. PL decay profiles of five InN samples with different free carrier concentrations.

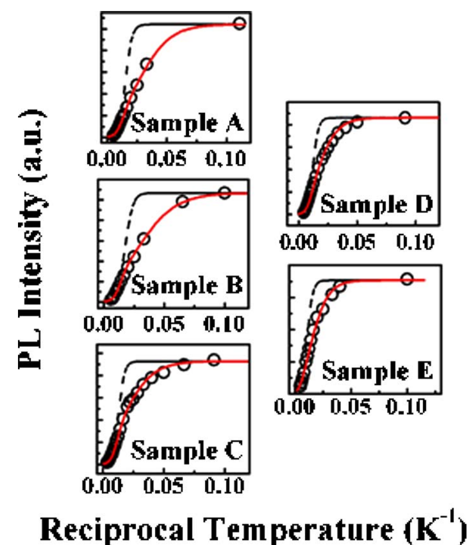

FIG. 4. (Color online) Arrhenius plot of the integrated PL intensity of five InN samples with different carrier concentrations (open circles). The solid lines are the fitted curves using Eq. (2).

Downloaded 19 Oct 2008 to 140.116.208.51. Redistribution subject to AIP license or copyright; see http://apl.aip.org/apl/copyright.jsp

$$I(T) = \frac{I(0)}{1 + A_1 \exp(-E_1/kT) + A_2 \exp(-E_2/kT)}, \quad (2)$$

where $I(0)$ is the PL intensity at low temperature, the coefficients A_1 and A_2 measure the strengths of both quenching mechanisms, and E_1 and E_2 are the thermal activation energies in the high- and low-temperature regions, respectively. The solid lines in Fig. 4 show the fitted results, which agree closely with the experimental data. In the fits, E_1 extracted from the high-temperature region (above 100 K) has an activation energy of ~30 meV, which is almost independent of the carrier concentration. We suggest that E_1 is caused by the nonradiative channel through defects or dislocations in InN. On the other hand, the open triangles of Fig. 3 plot activation energy E_2 that was extracted from the low-temperature region (10–100 K), revealing that E_2 increases with the carrier concentration. The carriers in the thermalization process may become delocalized from the localized states, leading to the decrease of PL intensity accordingly. The concentration-dependent E_2, which is close to the value of E_0, thus represents the localization energy of the localized carriers.

Two possible mechanisms have been suggested to explain the origin of the carrier localization in InN: the random impurity potential[5,6] and the metallic indium inclusions.[7] To determine whether the carrier localization in InN originates from the latter mechanism, the composition of the InN samples was examined by making the energy dispersive x-ray measurements. InN with a lower carrier concentration contains a greater atomic percentage of indium than that with higher carrier concentration. If carrier localization arises from the metallic indium inclusions, then the InN with the lower carrier concentration should exhibit strengthened localization. However, the localization energy in InN decreases as the carrier concentration decreases, as shown in Fig. 3, indicating that the mechanism based on the metallic indium inclusions was not responsible for the carrier localization here. We therefore suggest that the carrier localization in InN is associated with the potential fluctuation of the randomly located impurities. Based on this model, the localization energy can be estimated at different carrier concentrations. In heavily doped semiconductors, the inhomogeneous impurity distribution may produce a density-of-states tail by electron-impurity interactions. The localized states in such a bail tail can be treated as acceptor-type centers, distributed above the top of the valence band. If the randomness of ionic impurities produces potential fluctuations, then the root-mean-square (rms) potential energy fluctuation is given by[14]

$$V_{\rm rms} = (e^2/\varepsilon)[2\pi(N_D^+ + N_A^-)R_s]^{1/2}, \quad (3)$$

where ε is the dielectric constant, N_D^+ and N_A^- is the concentration of ionized donors and acceptors, respectively, R_s is the screening length, and $N_D^+ + N_A^- \cong n$ is the free electron concentration. In the case of a degenerate semiconductor, the screening length R_s is given by the Thomas-Fermi approximation:[6,14]

$$R_s \cong \frac{a_B}{2}(na_B^3)^{-1/6}, \quad (4)$$

where

$$a_B = \frac{\varepsilon}{4\pi e^2}\frac{\hbar^2}{m^*}$$

is the effective Bohr radius and m^* is the hole effective mass. Combining the Eqs. (3) and (4) and using $m^* = 0.3m_0$ (Ref. 6) yield the following expression: $V_{\rm rms} = 0.785 \times 10^{-10} n^{5/12}$ (eV). According to the analysis of Arnaudov *et al.*, the localization energy at low temperature is given by the potential fluctuation of the valence band tails:[6] $E_{\rm loc} \sim 2^{1/2} V_{\rm rms}$. Therefore, the localization energy in InN scales as the $n^{5/12}$ power of the carrier concentration. The solid line in Fig. 3 presents the calculated localization energy versus carrier concentration, which agrees closely with the experimental results.

In summary, the concentration-dependent localization energy of carriers is obtained from the emission-energy dependence of the PL decays and the PL quenching in thermalization. The localization energy increases with the carrier concentration. A model based on the transition between free electrons in the conduction band and localized holes in the deeper tail states is used to explain the concentration dependence of localization energy in InN.

This project was supported in part by the National Science Council of Taiwan under Grant Nos. NSC 94-2112-M-033-013 and NSC 94-2745-M-033-001-URD.

[1]J. Wu, W. Walukiewicz, K. M. Yu, J. W. Ager III, E. E. Haller, Hai Lu, William J. Schaff, Yoshiki Saito, and Yasushi Nanishi, Appl. Phys. Lett. **80**, 3967 (2002).
[2]V. Yu. Davydov, A. A. Klochikhin, R. P. Seisyan, V. V. Emtsev, S. V. Ivanov, F. Bechstedt, J. Furthmüller, H. Harima, A. V. Mudryi, J. Aderhold, O. Semchinova, and J. Graul, Phys. Status Solidi B **229**, R1 (2002).
[3]A. G. Bhuiyan, A. Hashimoto, and A. Yamamoto, J. Appl. Phys. **94**, 2779 (2003).
[4]K. S. A. Butcher and T. L. Tansley, Superlattices Microstruct. **38**, 1 (2005).
[5]A. A. Klochikhin, V. Yu. Davydov, V. V. Emtsev, A. V. Sakharov, V. A. Kapitonov, B. A. Andreev, Hai Lu, and William J. Schaff, Phys. Rev. B **71**, 195207 (2005).
[6]B. Arnaudov, T. Paskova, P. P. Paskov, B. Magnusson, E. Valcheva, B. Monemar, H. Lu, W. J. Schaff, H. Amano, and I. Akasaki, Phys. Rev. B **69**, 115216 (2004).
[7]R. Intartaglia, B. Maleyre, S. Ruffenach, O. Briot, T. Taliercio, and B. Gil, Appl. Phys. Lett. **86**, 142104 (2005).
[8]J. Wu, W. Walukiewicz, S. X. Li, R. Armitage, J. C. Ho, E. R. Weber, E. E. Haller, Hai Lu, William J. Schaff, A. Barcz, and R. Jakiela, Appl. Phys. Lett. **84**, 2805 (2004).
[9]F. Chen, A. N. Cartwright, H. Lu, and William J. Schaff, J. Cryst. Growth **269**, 10 (2004).
[10]T. Passow, K. Leonardi, H. Heinke, D. Hommel, D. Litvinov, A. Rosenauer, D. Gerthsen, D. Litvinov, A. Rosenauer, D. Gerthsen, J. Seufert, G. Bacher, and A. Forchel, J. Appl. Phys. **92**, 6546 (2002).
[11]E. Cohen and M. D. Sturge, Phys. Rev. B **25**, 3828 (1982).
[12]M. Strassburg, M. Dworzak, H. Born, R. Heitz, A. Hoffmann, M. Barteis, K. Lischka, D. Schikora, and J. Christen, Appl. Phys. Lett. **80**, 473 (2002).
[13]M. Leroux, N. Grandjean, B. Beaumont, G. Nataf, F. Semond, J. Massies, and P. Gibart, J. Appl. Phys. **86**, 3721 (1999).
[14]J. D. Sheng, Y. Makita, K. Ploog, and H. J. Queisser, J. Appl. Phys. **53**, 999 (1982).

Downloaded 19 Oct 2008 to 140.116.208.51. Redistribution subject to AIP license or copyright; see http://apl.aip.org/apl/copyright.jsp